

The Temperature Uniformity During Air Drying of a Colloidal Liquid Droplet

Kamlesh C. Patel, Xiao Dong Chen, and Saptarshi Kar

Department of Chemical and Materials Engineering, The University of
Auckland, Auckland, New Zealand

Abstract: The mathematical analysis for drying of individual droplets containing dissolved or suspended solids has been given significant importance due to the increasing popularity of the spray drying operation in the production of various chemicals, ceramics, drugs, food, and dairy powders as well as nanoparticles. The physical and biological qualities of the final products primarily depend on the history experienced by the droplet within the dryer. It is, therefore, desirable to ‘estimate’ the droplet’s behavior and various characteristics such as moisture content and temperature profiles accurately. In the literature, several models have been presented to estimate moisture and temperature profiles inside a particle considering various assumptions. One common assumption is the uniform temperature distribution within the droplets being dried. The present article has presented an estimation procedure to evaluate the temperature distribution within a porous skim milk droplet to determine whether the uniform temperature distribution assumption is reasonable. Here, the surface-center temperature differences were estimated by considering the one-dimensional, unsteady-state heat conduction equation for a spherical droplet. Shrinkage of droplets was taken into consideration during modeling. A new concept of the Biot number has also been applied in the current article to assist in the determination of the rate-limiting process.

Keywords: Droplet; Drying; Heat conduction; Modeling; Biot number; Surface temperature

Correspondence: Xiao Dong Chen, Department of Chemical and Materials Engineering, The University of Auckland, Private Bag 92019, Auckland 1001, New Zealand; Tel.: + 6493737599 × 87004; Fax: + 6493737463; E-mail: d.chen@auckland.ac.nz

INTRODUCTION

Spray drying is a very effective method of powder manufacturing in the food, dairy, chemical, agrochemical, biological, and pharmaceutical industries. It is a common drying as well as a preservation method in which the bulk liquid feed is transformed into a spray of very small droplets of the order of several hundred microns, exposing the droplets to a hot drying environment until the exit particles achieve the prerequisite quality. A simple approach for accomplishing the expected product quality is to recognize that the quality of the end product is the result of what a droplet or particle experiences (with respect to the temperature and moisture concentration) during its transit in the spray dryer and how it responds to these changes. For instance, the nutritional value of any food materials primarily depends on the temperature and moisture history of the droplet during processing. Therefore, it is essential to model the changes in droplet temperature and moisture concentration with respect to time. It should be noted that the surface properties and the quality of the final particles are also influenced by some operational variables such as feed flow rate, feed concentration, air temperature and air humidity.^[1] Recent studies illustrate that the computational fluid dynamics (CFD) approach is becoming popular in optimising and designing spray drying.^[2-5] An extensive research has been carried out using CFD packages to study the behavior of the performance of a spray dryer and to investigate the effects of operational variables.

In typical spray drying processes, the hot gas is mixed with the spray of individual droplets for the removal of excess moisture from the droplets. The droplet (low temperature phase) receives heat from the gas (relatively high temperature phase). Consequently, moisture is transferred from the droplets (high moisture concentration phase) to the gas (relatively low moisture concentration phase) in the form of vapor. The driving force may be the moisture concentration difference, the pressure difference, or the temperature difference. The transport of heat and moisture may lead to the nonuniformity of temperature, pressure, and moisture concentration inside the droplets depending on the type, size, constituents, and the form of the materials being dried. This nonuniformity can affect both the physical and biological characteristics of the particles during processing. For instance, the nonuniformity may influence physical properties such as stickiness, flowability, immersibility, wettability, dispersibility, and solubility, along with the nutritional values such as degradation of protein, enzyme, and vitamins within the particles and also the shelf-life of the bioactive products. Furthermore, the nonuniformity of temperature and moisture content may affect the drying kinetics as some parameters such as thermal diffusivity and mass diffusivity are

function of local conditions. However, the impact of the nonuniformity on the product quality and the drying kinetics primarily depends on the magnitude of the nonuniformity. Therefore, a more thorough understanding of modeling for the nonuniformity inside a droplet in drying applications is necessary as it helps to improve the product quality and also the spray dryer design.

In general, spray drying is a process that is believed to be a coupled heat and mass transfer operation. Modeling for drying of the single droplets requires the solution of coupled heat and mass transfer models. There have been many studies published in literature on modeling the transport processes during air drying of single droplets, particles or thin layer materials,^[6–20] especially with respect to hygroscopic materials such as food, paper, wood, etc. A better understanding of the controlling mechanisms in the heat and mass transfer processes under evaporation conditions is one of the fundamental tools in optimising the drying process and in determining the product quality. In most previous studies, models are formulated to characterise the transport processes assuming the process is mass transfer limiting or at least coupled heat and mass transfer limiting.^[7–10,12,14] On the other hand, Farid^[20] has made an argument for the heat transfer limiting process, assuming only the crust thermal conductivity controls the drying process. It has become an interesting research task to discover the controlling mechanisms of the droplet drying process and to select the appropriate formulae to represent the transport phenomena and properties.

Basic Modeling Approaches

In general, three modeling approaches are found in the literature based on the assumptions considered for modeling the heat and mass transfer during air drying of small droplets and porous particles. The first approach assumes that there is negligible temperature nonuniformity inside the droplets.^[6,13,16,21,22] The moisture concentration distribution effect is taken care of by the proposed lumped kinetics models.^[13,16,18] This approach is simple in application and is found to predict the changes in temperature and moisture concentration satisfactorily for the small droplets under the laboratory conditions. This kind of approach is widely used in modeling the large-scale operations, mainly due to the simplicity (as it requires only time integration) and fairly reasonable accuracy in the predictions of the drying parameters and the product quality. The moisture concentration profile was generally predicted using one of the effective drying kinetics models. The following heat transfer model was used to estimate the changes in particle temperature assuming Biot number

(*Bi*) is close to its critical value:

$$\frac{dT_p}{dt} = \frac{h \cdot A_p \cdot (T_b - T_p) + \Delta H_V \cdot (dm_w/dt)}{m_p \cdot C_{p_p}} \quad (1)$$

The second modeling approach assumes a uniform temperature within the small droplets but solves for the detailed moisture concentration distribution.^[7,9,12,14] The internal mass transfer was considered as a rate-limiting factor assuming the internal heat transport takes place quickly in comparison to the internal mass transport. The internal transport of liquid moisture for a spherical, shrinking droplet of binary systems was generally expressed using the unsteady state, one-dimensional, Fickian-type equation. The same heat transfer model was used as defined by Eq. (1) to evaluate the particle temperature. This approach was well accepted because it was found to correlate the experimental weight loss data reasonably well with the theoretical predictions. However, large errors were noted with the temperature predictions.

The third modeling approach takes into account the spatial temperature distribution inside a droplet.^[10,20,23] This modeling approach was based on the formation of solid crust from a preferential site, usually the droplet surface. As drying proceeds, the crust is assumed to be thickened forming a moving boundary or a receding interface. In general, the partially dried particle was divided into the two main regions: the outer dry crust and the inner wet core. In fact, several assumptions were made during estimation of the internal temperature distribution. For instance, Cheong et al.^[10] assumed a linear temperature distribution in the dry region of the material and a uniform temperature throughout the wet core, which may not be true for the spherical or cylindrical geometry. Farid^[20] has not considered the mass transfer resistance during modeling the internal heat transport. Furthermore, it was assumed that evaporation only occurs through a sharp moving boundary, a thin evaporation interface between the wet core and the dry crust. The temperature distribution was mainly calculated using the following heat conduction equation by taking into consideration two different regions having fixed moisture content:

$$\frac{\partial T}{\partial t} = \frac{\alpha}{r^2} \left[\frac{\partial}{\partial r} \left(r^2 \frac{\partial T}{\partial r} \right) \right] \quad (2)$$

Eq. (2) was solved with the following boundary conditions:

$$\frac{dT}{dr} = 0 \quad \text{at } r = 0, \quad (3)$$

$$-k \frac{dT}{dr} = h(T_s - T_b) \quad \text{at } r = R \quad (4)$$

where α is the thermal diffusivity of droplet and R is the droplet radius. The overall change in the weight of the droplet during drying was calculated assuming the mass of solids and the mass of ‘bound’ water remain constant during the entire drying period. The weight of the droplet was then expressed in terms of the mass of solids, bound water and free water using the following equation:^[20]

$$\text{Mass} = \frac{4}{3}\pi R^3 \rho_p (1 - w_0) + \frac{4}{3}\pi R^3 \rho_p (w_0 - w_b) + \frac{4}{3}\pi R^3 \rho_p w_b \quad (5)$$

The first and the third term on the right-hand side of Eq. (5) represent the mass of solids and bound water, respectively. The second term represents the mass of free water in the core region, which was considered to be available for the removal. Hence, there was no drying kinetics involved during modeling of the change in mass of the droplets. The models have shown reasonable agreements between the predicted and the measured weight loss profiles. Nevertheless, large errors were noted in the average temperature predictions for air drying of the 20 wt% skim milk droplets of 1.9 mm initial diameter.

Analysis of the Temperature Distribution Models

During modeling of small droplets under drying conditions, a range of assumptions were introduced. One common assumption was negligible temperature nonuniformity inside a small droplet. The intention of introducing this assumption was to simplify the mathematical analysis, to reduce the computation time and to make the drying models more compatible for the commercial CFD programs such as Fluent. The theoretical justification of this assumption requires the estimation of temperature distribution and Biot number. For the uniform temperature assumption to be correct, Biot number should be less than the critical value of 0.1.^[20,24–26] For a spherical, ‘non-evaporative’ droplet, Biot number is usually defined by considering the convective heat flux through the surface equal to the conduction heat flux within the material. The Biot number can be expressed in terms of the ratio of the internal resistance to the external resistance as:

$$Bi = \frac{\bar{h} \cdot R}{\bar{k}_p} \quad (6)$$

In the above equation, the parameter \bar{h} is the average heat transfer coefficient for convection over the entire surface, \bar{k}_p is the mean thermal conductivity of the particle and R is the droplet radius. At the beginning of the drying process, the Biot number is likely to be small due to the

larger thermal conductivity because the droplet has a high amount of water. After some period of drying, a major portion of water is transferred from the droplet to the gas phase, lowering the thermal conductivity of the partially moist droplet. Another reason for the reduced thermal conductivity is the increment in the porosity of a particle possibly filled with air and/or vapour, which have the low thermal conductivity value. Since the Biot number is inversely proportional to the mean thermal conductivity of the particle, it is expected to become larger. It is, therefore, possible that Biot number could exceed the critical value of 0.1 (which is a convenient value chosen in the classical texts) and consequently the temperature gradient inside a particle could not be ignored.

Several models were formulated in the literature for estimating the temperature gradient within the materials under drying conditions.^[10,20,23] Most of the work published to date is based on the moving boundary or the receding interface approach. For instance, as mentioned earlier, Farid^[20] has recently published a moving boundary model for air drying of small droplets, which was discussed here in detail. The model was constructed based on a heat-transfer limiting theory, which believes that drying is heat-transfer limiting assuming only the crust thermal conductivity controls the drying process. The entire drying process for a single droplet was partitioned into four distinct process stages, as shown in Fig. 1. The first process stage was the initial wet-bulb temperature adjustment in which the droplet surface temperature reached the air wet-bulb temperature. Equation (2) was solved using the boundary conditions described by Eqs. (3) and (4) to estimate the temperature distribution. The evaporation rate was assumed to be zero during this

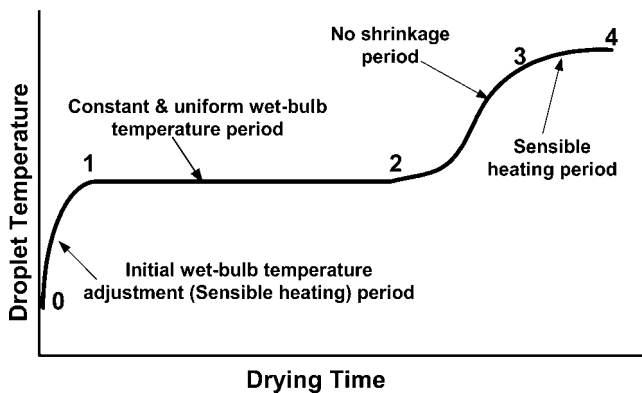


Figure 1. The four stages of drying of a droplet in the heat transfer limiting approach.

wet-bulb temperature adjustment considering sensible heating. During the second process stage, the droplet had to experience evaporation until the free moisture on the droplet surface was zero. The temperature of the droplet was assumed to remain at the corresponding wet-bulb temperature of surrounding air throughout the second stage. Furthermore, a uniform temperature within the droplet was assumed during this constant wet-bulb temperature period. The droplet had to experience shrinkage during this period only.

After the constant-temperature (also known as the uniform temperature) period, the crust formation was commenced on the droplet surface and shrinkage was believed to be stopped. Thus, the partially dried droplet was divided into the two main regions, the outer dry crust and the inner wet core, separated by a sharp moving boundary. Evaporation was assumed to occur only from this moving boundary. The model was formulated based on the theory that the dry crust has constant 'bound' moisture content, which cannot be removed further, whilst the moving boundary and the wet core were assumed to be at the saturated conditions until the centre point reached the same 'bound' moisture content. The same heat conduction equation (Eq. 2) was solved using the same boundary conditions (Eqs. (3) and (4)) for the dry crust and the wet core, which had the previously set moisture concentrations. The third process stage of drying lasted until the dry crust reached the centre of the particle and then drying was assumed to be finished. The final and fourth stage was set for another sensible heating of the completely dry particle. During this final stage, the temperature distribution inside a dried particle was estimated using Eqs. (2) to (4) considering only the crust thermophysical properties.

The first two drying stages of the heat transfer limiting theory considered by Farid^[20] can be summarized with respect to the droplet temperature as discussed in this paragraph. The droplet was at a uniform temperature under the absence of hot air. During the first stage of sensible heating period, the droplet surface temperature reached the air wet-bulb temperature but the droplet center temperature was still the same as the initial droplet temperature. Some temperature difference was expected between the center and the surface temperatures. Then, after the wet-bulb temperature adjustment, the droplet was assumed to achieve the uniform temperature (no temperature gradient), which was equal to the air wet-bulb temperature. The centre temperature was increased up to the surface temperature during this process stage. The droplet temperature was also assumed to remain constant until zero free moisture on the droplet surface. However, the predicted temperature profiles for the 20 wt% skim milk droplets in Farid^[20] show that the droplet temperature was not constant after the wet-bulb temperature adjustment period. In other words, the predictions were inconsistent with the theory developed.

It is common in the industries to spray the skim milk droplets with 50 wt% initial solids content and 50–60°C initial droplet temperature. For the droplets having a high initial temperature (higher than the air wet-bulb temperature), the droplet surface temperature has to be reduced until the air wet-bulb temperature is achieved. The reduction of the surface temperature requires some evaporation on the droplet surface during this wet-bulb temperature adjustment. This impression is supported by the experimental work of Cheong et al.^[10] and Lin^[27] on drying of the liquid droplets, which contain solids. Therefore, the consideration of no evaporation during the first process stage of drying by the heat-transfer limiting theory may not be appropriate, especially for simulating drying of the droplets having high initial temperature. Further, there would be a negligible uniform-temperature period for materials with a high initial solids content (very little constant-rate drying period) because the surface temperature would rise continuously (and quickly) due to the very small moisture content on the droplet surface.^[16] Therefore, the first two process stages would only exist for the pure water droplets or droplets that have high initial moisture contents.

At the beginning of the third stage of drying, shrinkage was assumed to be stopped due to the formation of a solid crust on the droplet surface. It is, however, shown that shrinkage occurs throughout the drying of skim milk or whole milk droplets in the laboratory conditions examined.^[28] The surface properties (moisture content and temperature) of the droplet/particle are believed to play an important role for the continuous reduction in the droplet size during drying. The surface, however, may be fixed during very high temperature drying conditions. Once the crust formed, the dry crust was further assumed to have small and constant bound water, irrespective of the air humidity. The heat-transfer limiting approach has predetermined the surface water concentration. Therefore, this concept does not correspond to the principle of the equilibrium moisture content.^[11,16,29]

An abrupt drop in moisture concentrations at the moving boundary was expected because the wet core (and the moving boundary) were considered to have saturated water concentrations while the dry crust had constant (very small) bound water content. Since materials like skim milk solids have a high affinity to absorb moisture (highly hygroscopic), some moisture concentration distribution is expected between the dry outer surface and the saturated core.^[19] Reis et al.^[30] studied the moisture profile in a model food droplet during drying using a magnetic resonance imaging technique and confirmed that there is no sharp interface between the wet and the dry regions on which evaporation occurs. Cheong et al.^[10] assumed that evaporation occurs only on a sharp interface during modeling of drying of aqueous sodium sulphate decahydrate solution. The

simulated results of Cheong et al.^[10] illustrate that the formulated model has overestimated the droplet weight profile after the crust has formed on the droplet surface. This means, the measured droplet weight after the crust formation was smaller than the predicted one. This implies that evaporation should occur in a certain region between the droplet outer surface and the wet saturated core rather than on a sharp interface only. These findings invalidate the consideration of evaporation through a sharp moving boundary or receding interface after the crust formation.

Whitaker^[30] studied the gas-phase convective transport during drying of porous media and shown that the moisture flux should be present in the dry crust region having certain moisture content. This phenomenon is supported by Chen and Pei,^[11] who proposed that water may move within the crust due to the flow along very fine capillaries or through the cellular membranes during drying of hygroscopic materials. This movement of water generates a transitional moisture distribution in the crust region. Further, it was shown that bound water could not be constant as some bound water molecules receive enough energy to break the sorptive bonds.^[32] These free molecules may migrate until captured by the other sites or may be evaporated. These experimental studies show that the assumptions of evaporation through a sharp moving boundary and a constant and linear bound water profile in the crust region, as considered by the heat transfer limiting theory, are not appropriate during modeling the temperature distribution within the droplet.

The heat transfer limiting theory had assumed, based on the Biot number estimation, that the drying of small droplets is controlled by the crust thermal conductivity only. For the 20 wt% skim milk droplet of 1.9 mm initial diameter, Farid^[20] used the initial thermal conductivity as $0.55 \text{ W} \cdot \text{m}^{-1} \cdot \text{K}^{-1}$ (essentially the thermal conductivity of pure water) during calculation of the Biot number, which was shown to be around 0.15. As drying progressed, the author illustrated that Biot number was increased by one order of magnitude (higher than the value of 1) by setting the value of thermal conductivity as $0.07 \text{ W} \cdot \text{m}^{-1} \cdot \text{K}^{-1}$. The values of thermal conductivities for the skim milk particles used in modeling work by Farid^[20] may truly be on the low side. In addition, the author used the same definition of the Biot number, illustrated in Eq. (6), for droplets under nonevaporative and evaporative conditions to determine the rate-controlling factor for the droplet drying process.

Objectives

The temperature distribution and Biot number information can be helpful to determine the rate-limiting process and also to justify the uniform

temperature assumption. The analysis of temperature distribution models has shown that the modeling approach similar to the heat-transfer limiting theory (the moving boundary model) or the receding interface approach have many limitations and they may not provide accurate predictions for all situations. The main objective of the present study is to formulate a model to explore a more realistic extent of the temperature distribution within a particle during air drying. In literature, the conventional concept of Biot number, defined by Eq. (6), has been used during modeling the droplet drying process. However, this concept does not account for the evaporation effects and may not represent the true scenario. The present study has introduced a new concept of Biot number for the small droplets under evaporation conditions. During modeling of the temperature distribution, a more rational approach for evaluating the mean thermal conductivity of single droplets has been developed. Simulation has been carried out by incorporating the measured weight loss and temperature data into the formulated models.

BIOT NUMBER ANALYSIS

In this article, the Biot number is modified for the evaporative droplets considering the heat-source term along with the internal and external heat transfer terms. A new Biot number was developed by considering a steady-state energy balance over a droplet experiencing drying:

$$\bar{h} \cdot (T_b - T_s) - \Delta H_v \cdot \hat{N}_v = \bar{k}_p \cdot \frac{T_s - T_c}{R} \quad (7)$$

where ΔH_v is the latent heat of vaporisation (J/kg), \hat{N}_v is the surface-based evaporation rate (kg/m²·s), T_b is the bulk-gas phase temperature (K) and T_s and T_c are the droplet surface and centre temperatures (K), respectively. To evaluate the Biot number, Eq. (7) can be written in terms of an equivalent heat transfer coefficient as:

$$\bar{h} \cdot (T_b - T_s) - \Delta H_v \cdot \hat{N}_v = \bar{h}^* \cdot (T_b - T_s) = \bar{k}_p \cdot \frac{T_s - T_c}{R} \quad (8)$$

where \bar{h}^* is the equivalent convection heat transfer coefficient. From Eq. (8), the equivalent convection heat transfer coefficient (\bar{h}^*) can be expressed as:

$$\bar{h}^* = \bar{h} - \frac{\Delta H_v \cdot \hat{N}_v}{(T_b - T_s)} \quad (9)$$

On multiplication of both sides of Eq. (9) with (R/\bar{k}_p) , we have

$$\frac{\bar{h}^* \cdot R}{\bar{k}_p} = \frac{\bar{h} \cdot R}{\bar{k}_p} - \frac{\Delta H_v \cdot \hat{N}_v}{(T_b - T_s)} \cdot \frac{R}{\bar{k}_p} \tag{10}$$

Thus, the new Biot number, which has taken into account the drying effects, can be expressed as:

$$Bi(\text{new}) = Bi - \frac{\Delta H_v \cdot \hat{N}_v}{(T_b - T_s)} \cdot \frac{R}{\bar{k}_p} \tag{11}$$

where $Bi(\text{new})$ is a new Biot number and Bi is a conventional Biot number. The second term on the right hand side of Eq. (11) should be considered when evaporation plays a considerable role in the removal of moisture. The Biot number analysis shows that the Biot number not only depends on the average heat-transfer coefficient, droplet radius and droplet thermal conductivity. It also depends on the average drying rate and the difference between the gas and the surface temperatures. Based on this new definition, new Biot numbers are expected to be smaller than those estimated using the conventional theory. Further, Chen and Peng^[19] proposed that the critical Biot number for the uniform temperature assumption could be larger than the value of 0.1 when significant evaporation is involved. Based on the Biot number theory proposed here, the differences between the surface and the center temperatures may not be as large as perceived in the conventional approach to the non-drying situations.

MATHEMATICAL MODEL

The model is formulated here to estimate the temperature nonuniformity within a droplet, based on the perception that the evaporation front is not a sharp one. Drying starts with evaporation of excess (free) moisture on the droplet surface. When the droplet surface is fully covered with water, the drying rate would be similar to the rate for pure water evaporation. When a droplet containing dissolved or suspended solids is being dried, the vapour pressure at the droplet surface becomes smaller than that of the pure water droplet as evaporation proceeds. As a result, the mass transfer rate will be reduced during drying of the droplet. The surface temperature of the evaporating droplet will consequently increase to be above the wet-bulb temperature or the evaporation temperature of the pure water droplet. The drying characteristics will be related to the formation of a porous solid phase at the surface of the droplet. Once the surface vapor concentration falls below the saturated vapor concentration

corresponding to the surface temperature, drying will also commence within the droplet. The flow of heat and moisture would lead to a temperature gradient within the droplet being dried. The temperature gradient can be evaluated by balancing the heat for a droplet-air system. The energy balance can be written for a spherical droplet under evaporation conditions using the spherical coordinate system (r, t) considering the one-dimensional, homogeneous, unsteady state, effective heat conduction equation:

$$\frac{1}{r^2} \frac{\partial}{\partial r} \left(k_p \cdot r^2 \frac{\partial T}{\partial r} \right) + \overline{\Delta H}_v \cdot \overline{E}_v = \overline{\rho} \cdot \overline{C}_p \cdot \frac{\partial T}{\partial t} \quad (12)$$

where k_p is the thermal conductivity of droplet, \overline{E}_v is the volume-based evaporation rate (which is negative when evaporation occurs), $\overline{\rho}$ is the average particle density, \overline{C}_p is the average heat capacity of the particle and $\overline{\Delta H}_v$ is the latent heat of water vaporisation. In the present study, thermal conductivity was estimated and averaged along the droplet radius during simulation. If we use the integrated mean thermal conductivity (\overline{k}_p) along the droplet/particle radius, we can rewrite the above equation as:

$$\overline{\rho} \cdot \overline{C}_p \cdot \frac{\partial T}{\partial t} = \frac{\overline{k}_p}{r^2} \frac{\partial}{\partial r} \left(r^2 \frac{\partial T}{\partial r} \right) + \overline{\Delta H}_v \cdot \overline{E}_v \quad (13)$$

Dividing both sides of the above equation with the mean thermal conductivity results in the following:

$$\frac{\overline{\rho} \cdot \overline{C}_p}{\overline{k}_p} \cdot \frac{\partial T}{\partial t} = \frac{1}{r^2} \frac{\partial}{\partial r} \left(r^2 \frac{\partial T}{\partial r} \right) + \frac{\overline{\Delta H}_v \cdot \overline{E}_v}{\overline{k}_p} \quad (14)$$

The physical significance of the thermal diffusivity is associated with the speed of propagation of heat into the solid during changes of temperature with time. The higher the thermal diffusivity, the shorter is the time required for the applied heat to penetrate into the depth of the solid. The average thermal diffusivity can be defined as:

$$\overline{\alpha} = \frac{\overline{k}_p}{\overline{\rho} \cdot \overline{C}_p} \quad (15)$$

By introducing the thermal diffusivity term in Eq. (14), we have

$$\frac{1}{\overline{\alpha}} \cdot \frac{\partial T}{\partial t} = \frac{1}{r^2} \frac{\partial}{\partial r} \left(r^2 \frac{\partial T}{\partial r} \right) + \frac{\overline{\Delta H}_v \cdot \overline{E}_v}{\overline{k}_p} \quad (16)$$

As we are interested in estimating the temperature distribution within a droplet, we may want to follow the temperature inside a droplet with respect to the radius. The measured temperature is taken as an average temperature of the droplet/particle, though it is possible that during the earlier stages of drying when the droplet is more perfect and the thermocouple is at the center, the measured temperature would be closer to the core temperature. We can plot the average measured temperature $T_p (= \bar{T})$ against time t to get the temperature increment with respect to time ($\partial T_p / \partial t$). For an individual time step, the second term and the third term of Eq. (16) can be considered to be constant, as long as we use the average values for the latent heat of vaporization and the drying rate. Under these circumstances, Eq. (16) can be written as:

$$\frac{1}{r^2} \frac{\partial}{\partial r} \left(r^2 \frac{\partial T}{\partial r} \right) + \left[\frac{\overline{\Delta H_v} \cdot \bar{E}_v}{\bar{k}_p} - \frac{1}{\bar{\alpha}} \cdot \frac{\partial T_p}{\partial t} \right] \approx 0 \tag{17}$$

If we multiply both sides of the Eq. (17) by ($r^2 dr$), we obtain Eq. (17) in its integral form:

$$\int \frac{\partial}{\partial r} \left(r^2 \frac{\partial T}{\partial r} \right) dr + \left[\frac{\overline{\Delta H_v} \cdot \bar{E}_v}{\bar{k}_p} - \frac{1}{\bar{\alpha}} \cdot \frac{\partial T_p}{\partial t} \right] \int r^2 dr \approx 0 \tag{18}$$

On integration of Eq. (18), we have:

$$r^2 \frac{\partial T}{\partial r} + \left[\frac{\overline{\Delta H_v} \cdot \bar{E}_v}{\bar{k}_p} - \frac{1}{\bar{\alpha}} \cdot \frac{\partial T_p}{\partial t} \right] \cdot \frac{r^3}{3} = C_1 \tag{19}$$

C_1 is the integration constant and can be obtained using a boundary condition. The first boundary condition is the same as that defined in Eq. (3):

$$\text{B.C.1: when } r = 0, \quad \frac{\partial T}{\partial r} = 0 \quad \text{and} \quad T = T_c$$

The parameter T_c is the drop centre temperature. On application of the first boundary condition, we find $C_1 = 0$. If we insert the value of the constant C_1 and divide Eq. (19) by r^2 , we can re-write Eq. (19) in the following integral form:

$$\int \frac{\partial T}{\partial r} dr + \left[\frac{\overline{\Delta H_v} \cdot \bar{E}_v}{\bar{k}_p} - \frac{1}{\bar{\alpha}} \cdot \frac{\partial T_p}{\partial t} \right] \cdot \int \frac{r}{3} dr = 0 \tag{20}$$

On integration of Eq. (20), we have:

$$T + \left[\frac{\overline{\Delta H}_v \cdot \overline{E}_v}{\overline{k}_p} - \frac{1}{\overline{\alpha}} \cdot \frac{\partial T_p}{\partial t} \right] \cdot \frac{r^2}{6} = C_2 \quad (21)$$

On application of the first boundary condition, we find the integration constant $C_2 = T_c$. Then, Eq. (21) can be presented as:

$$T(r) = T_c - \left[\frac{\overline{\Delta H}_v \cdot \overline{E}_v}{\overline{k}_p} - \frac{1}{\overline{\alpha}} \cdot \frac{\partial T_p}{\partial t} \right] \cdot \frac{r^2}{6} \quad (22)$$

This model, presented by Eq. (22), represents a second-order profile of temperature within the droplet/particle. Furthermore, the model would provide the droplet surface temperature when $r = R$. Hence, it is possible to estimate the maximum temperature difference, the difference between the surface and the centre temperatures, in a single droplet/particle over the entire drying period. This maximum temperature difference can be calculated using the following equation:

$$\Delta T_{\max} = T_s - T_c = \left[\frac{1}{\overline{\alpha}} \cdot \frac{\partial T_p}{\partial t} - \frac{\overline{\Delta H}_v \cdot \overline{E}_v}{\overline{k}_p} \right] \cdot \frac{R^2}{6} \quad (23)$$

During calculations, the average measured temperature and the average measured drying rate were used for the predictions of differences between the surface and the center temperatures. The experimental measurements were obtained for drying of skim milk droplets under different drying conditions.

In this study, the “mean” thermal conductivity was used to estimate Biot numbers as well as the temperature differences between the surface and the core temperatures. The thermal conductivity (k_p) of a small single particle is difficult to measure by the independent experiments. The model is formulated here to estimate the mean thermal conductivity by quantifying the fundamental constituents of the materials being dried. The present analysis has been carried out with skim milk because thermo-physical properties correlations and other experimental data are readily available in the literature for skim milk. Skim milk is a complex biological fluid made of many basic constituents. For analysis purpose, skim milk powder was considered to be made of the constituents, listed in Table 1 (provided by The Canadian Dairy Commission). The average value of each constituent in a single particle is determined based on the values published in other literatures.^[29,33]

In this work, the model is developed to estimate the mean thermal conductivity of a single droplet based on the effective approach

Table 1. Composition of skim milk powder

Component	Average range (wt%)	Mean (wt%)
Water	3–4	4.0
Carbohydrates	49.5–52.0	51.0
Fat	0.6–1.25	1.0
Protein	34.0–37.0	35.5
Ash	8.2–8.6	8.5
Total		100

considered by Chen and Peng,^[19] Bylund,^[33] Choi and Okos,^[34] Rahman,^[35] and Krokida et al.^[36] Considering the skim milk particle as a mixture of constituents listed in Table 1, the mean thermal conductivity can be calculated using the following series and parallel models:^[19,34]

A series model:

$$k_{\text{mixture}} = \varepsilon_{\text{water}} \cdot k_{\text{water}} + \varepsilon_{\text{protein}} \cdot k_{\text{protein}} + \varepsilon_{\text{fat}} \cdot k_{\text{fat}} + \varepsilon_{\text{carbohydrate}} \cdot k_{\text{carbohydrate}} + \varepsilon_{\text{ash}} \cdot k_{\text{ash}} \tag{24a}$$

A parallel model:

$$\frac{1}{k_{\text{mixture}}} = \frac{\varepsilon_{\text{water}}}{k_{\text{water}}} + \frac{\varepsilon_{\text{protein}}}{k_{\text{protein}}} + \frac{\varepsilon_{\text{fat}}}{k_{\text{fat}}} + \frac{\varepsilon_{\text{carbohydrate}}}{k_{\text{carbohydrate}}} + \frac{\varepsilon_{\text{ash}}}{k_{\text{ash}}} \tag{24b}$$

The rational value is likely to happen in between the above two limits. In the present study, the arithmetic average of the series and parallel values were used as a final value. The distribution factors were not incorporated because they needed to be evaluated using a regression method based on the experimental measurements. The arithmetic average is assumed to provide an estimate with negligible errors. In the above equations, ε_i is the volume fraction of each constituent (i). The volume fraction can be determined using the densities and the mass fraction values for the individual constituent:

$$\varepsilon_i = \frac{\omega_i \cdot \rho}{\rho_i} \tag{25}$$

where ω_i is the mass fraction of each constituent (wt%), ρ_i is the individual density ($\text{kg} \cdot \text{m}^{-3}$) and ρ is the overall mixture or particle density ($\text{kg} \cdot \text{m}^{-3}$). The particle density can be calculated as:

$$\rho = \frac{1}{\sum X_i / \rho_i} \tag{26}$$

The thermal conductivity of individual constituent can be estimated using the following correlations:^[19,34]

$$k_{\text{water}} = 0.57109 + 0.0017625 \cdot T - 6.7036 \times 10^{-6} \cdot T^2 \quad (27a)$$

$$k_{\text{protein}} = 0.17881 + 0.0011958 \cdot T - 2.7178 \times 10^{-6} \cdot T^2 \quad (27b)$$

$$k_{\text{fat}} = 0.18071 + 0.0027604 \cdot T - 1.7749 \times 10^{-7} \cdot T^2 \quad (27c)$$

$$k_{\text{carbohydrate}} = 0.20141 + 0.0013874 \cdot T - 4.3312 \times 10^{-6} \cdot T^2 \quad (27d)$$

$$k_{\text{ash}} = 0.32962 + 0.0014011 \cdot T - 2.9069 \times 10^{-6} \cdot T^2 \quad (27e)$$

Here, T is the local absolute temperature ($^{\circ}\text{C}$) and k is the thermal conductivity of the individual constituent ($\text{W}\cdot\text{m}^{-1}\cdot\text{K}^{-1}$).

The density ($\text{kg}\cdot\text{m}^{-3}$) of individual constituent was correlated with the local temperature (T , $^{\circ}\text{C}$) using the following equations:^[19,34]

$$\rho_{\text{water}} = 997.18 + 0.0031439 \cdot T - 0.0037574 \cdot T^2 \quad (28a)$$

$$\rho_{\text{protein}} = 1329.9 - 0.5185 \cdot T \quad (28b)$$

$$\rho_{\text{fat}} = 925.59 - 0.41757 \cdot T \quad (28c)$$

$$\rho_{\text{carbohydrate}} = 1599.1 - 0.31046 \cdot T \quad (28d)$$

$$\rho_{\text{ash}} = 2423.8 - 0.28063 \cdot T \quad (28e)$$

The mean thermal conductivity of the skim milk solids (k_s) can be estimated using Eqs. (24) to (28). The mean thermal conductivity of the reconstituted skim milk droplet (a mixture of solids and water) can be taken as an arithmetic average of the thermal conductivities calculated using the following series and parallel equations:

$$k_p = \varepsilon_{\text{water}} \cdot k_{\text{water}} + (1 - \varepsilon_{\text{water}}) \cdot k_s \quad (29a)$$

$$\frac{1}{k_p} = \frac{\varepsilon_{\text{water}}}{k_{\text{water}}} + \frac{1 - \varepsilon_{\text{water}}}{k_s} \quad (29b)$$

The same model can be used to estimate the mean thermal conductivity of the dried particle if the air effect can be neglected. When the influence of air is significant (i.e., higher porosity conditions), the thermal conductivity of the dried particle can be estimated considering the air porosity

and the air thermal conductivity as:

$$k_p = \epsilon_{\text{water}} \cdot k_{\text{water}} + (1 - \epsilon_{\text{water}} - \epsilon_{\text{air}}) \cdot k_s + k_{\text{air}} \cdot \epsilon_{\text{air}} \tag{30a}$$

$$\frac{1}{k_p} = \frac{\epsilon_{\text{water}}}{k_{\text{water}}} + \frac{1 - \epsilon_{\text{water}} - \epsilon_{\text{air}}}{k_s} + \frac{\epsilon_{\text{air}}}{k_{\text{air}}} \tag{30b}$$

The arithmetic average of the thermal conductivities estimated using Eqs. (30a) and (30b) can be used when calculating the Biot numbers for the dried particles. The porosity of the particle is, however, a complex function of the temperature, moisture content and the type of material. For dried particles of skim milk, the porosity is approximately 0.163 at 50°C conditions.^[37] The parameter (ΔH_v) in Eq. (23) is the integrated average value of the latent heat. The latent heat of vaporisation (ΔH_v , J/kg) was estimated at atmospheric pressure conditions using the following Watson correlation:^[38]

$$\frac{\Delta H_{v2}}{\Delta H_{v1}} = \left(\frac{1 - (T_2/T_c)}{1 - (T_1/T_c)} \right)^{0.38} \tag{31}$$

where T is the absolute temperature (K) and T_c is the critical temperature (K). Subscripts 1 and 2 describe the reference and the absolute conditions, respectively. It is known that at temperature $T = 273.15$ K, $\Delta H_v = 2500 \times 10^3$ J · kg⁻¹.^[29] This condition was used as a reference condition in Eq. (31) to estimate the latent heat of vaporization.

RESULTS AND DISCUSSION

The formulated models were solved using a first-order finite difference method. In this study, predictions are made using the experimental measurements of Lin.^[27] The simulations presented here are for drying of the 30 wt% skim milk droplets using three different sets of the drying conditions. The standard variations in measured droplet temperature and droplet diameter were noted as $\pm 0.1^\circ\text{C}$ and ± 0.02 mm,^[27] respectively. The initial droplet temperatures for sets one, two and three were 28.6, 31.8, and 30.8°C, respectively. The initial droplet diameter was 1.45 mm while the hot air used for drying had a velocity of 0.45 m/s and humidity of 0.0001 kg/kg (dry basis) during drying of the droplets using the constant air conditions. The air dry-bulb temperatures for sets one, two and three were 67.5, 87.1, and 106.6°C, respectively, and the corresponding wet-bulb temperatures were 23.4, 28.5, and 32.0°C, respectively. All other thermophysical properties were transient and either calculated using the appropriate correlations or measured from the corresponding

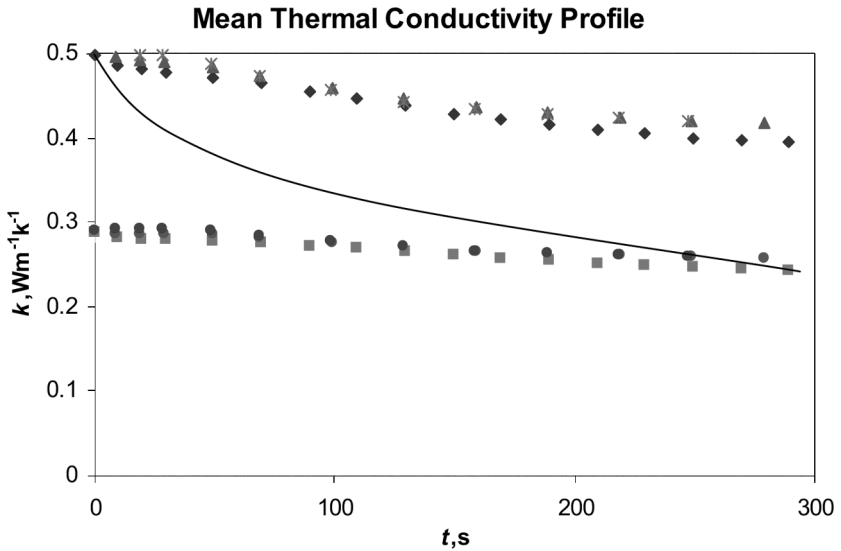


Figure 2. The mean thermal conductivity profiles for the 30 wt% (dry basis) skim milk droplet using sets one, two, and three drying conditions with and without considering the air phase in the particle.

experiments. Shrinkage in droplet size was not ignored during simulation of the droplet characteristics.

The mean thermal conductivity profiles of the drying droplets were estimated using the two models, one that does not consider the air phase in the particle structure and another that accounts for the air porosity, presented by Eqs. (29) and (30), respectively. We have used two models to calculate the thermal conductivity because it is extremely difficult to evaluate the transient changes in porosity within a single droplet during processing. Figure 2 illustrates the mean thermal conductivity profiles estimated using Eqs. (29) and (30) for the three sets of drying conditions, mentioned earlier in this section. The thermal conductivity models have predicted a gradual change in the thermal conductivity along the drying period. The mean thermal conductivity profiles estimated by Eq. (29), which does not consider the porosity term, illustrates that the mean thermal conductivity of the skim milk droplets at the beginning of drying was predicted as $0.50 \text{ W} \cdot \text{m}^{-1} \cdot \text{K}^{-1}$, while it was approximately $0.41 \text{ W} \cdot \text{m}^{-1} \cdot \text{K}^{-1}$ at the end of drying. Since the porosity of the droplet at the beginning of the drying process is negligible, the model presented by Eq. (29) would provide accurate values for the initial stages of drying. Furthermore, the temperature profiles would show the lower bounds for the surface-centre

temperature differences because the air phase was not considered in the solid structures during estimation of the mean thermal conductivity.

The mean thermal conductivity profiles, predicted using a model (Eq. (30)), which considers an air phase in the particle structure, are also depicted in Fig. 2 for the same experimental conditions. Since it is extremely difficult to evaluate the transient changes in the porosity for a single small-size droplet during drying, the model (Eq. (30)) in the present study has integrated the air porosity term from the beginning of the drying process. This would give an estimate of the mean thermal conductivity when the air effect cannot be neglected. Furthermore, this model would predict a low thermal conductivity from the beginning of the drying process. The low thermal conductivity would yield a higher bound of the surface-centre temperature differences. It can be seen from the profiles that the mean thermal conductivity of single skim milk droplets was $0.3 \text{ W} \cdot \text{m}^{-1} \cdot \text{K}^{-1}$ at the beginning of the process, while it was approximately $0.25 \text{ W} \cdot \text{m}^{-1} \cdot \text{K}^{-1}$ at the end of drying. It is to be noted that this model (Eq. (30)), which accounted for air porosity, would provide accurate values for the later stages of drying, because the porosity at the end of drying is very close to the value chosen in this study. In other terms, the model presented by Eq. (30) would underestimate the thermal conductivity during the earlier stages and hence it definitely overestimates the temperature differences during the earlier stages of drying.

The actual thermal conductivity profile would fall between the higher and lower bounds of the thermal conductivities shown in Fig. 1. The trend of the actual thermal conductivity profile for a drying droplet should be similar to a full line traced in Fig. 2. It would be interesting to evaluate the surface-centre temperature differences for particles having higher and lower mean thermal conductivity ranges. The higher range of mean thermal conductivity would yield the lower bound of the temperature differences while the lower range of mean thermal conductivity would result in the higher bound of the temperature differences. The measured droplet moisture content profiles and the higher and lower bounds of the surface-center temperature differences are depicted in Figs. 3 to 6. The true temperature difference is likely to be happen between the higher and lower bounds. A model, presented by Eq. (23), was used to estimate the surface-center temperature differences (ΔT_{max}).

It becomes clear, from Figs. 3 to 6, that the differences between the surface and the centre temperatures were small and not as large as predicted by the heat-transfer limiting theory. For instance, the heat-transfer limiting model predicted approximately 12°C surface-core temperature differences for the 20 wt% skim milk droplets having an initial diameter of 1.9 mm with drying at 70°C air temperature and 1.0 m/s air velocity conditions.^[20] In contrast, the analysis given here in this paper shows that

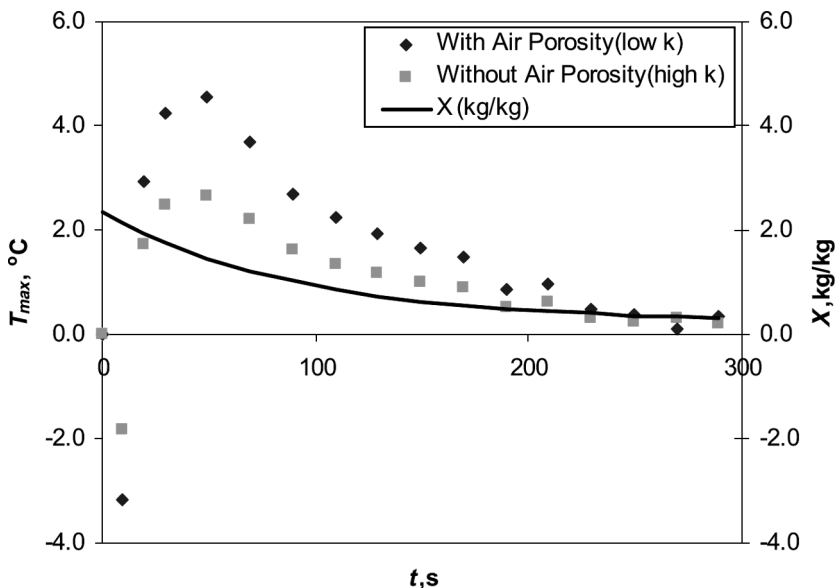


Figure 3. The surface-center temperature difference profiles for the 30 wt% (dry basis) skim milk droplet of 1.45 mm initial diameter and 28.6°C initial temperature during drying with hot air of 67.5°C dry-bulb temp, 23.4°C wet-bulb temp, and 0.45 m/s velocity (set one conditions).

the maximum temperature difference was 2.7°C and 4.5°C (refer Fig. 3) using the high and low thermal conductivity bounds, respectively, for the 30 wt% skim milk droplets of 1.45 mm initial diameter using the 67.5°C air temperature and 0.45 m/s air velocity conditions. The magnitude of temperature distribution estimated here is comparatively small. However, the air velocity considered in the set one drying conditions was half of the air velocity used by the heat-transfer limiting theory.^[20] The temperature differences are also predicted here for the experimental data using the 67.5°C air temperature and 1.0 m/s air velocity conditions with the same skim milk droplets characteristics mentioned in the set one drying conditions. Figure 4 illustrates that the maximum temperature difference was 4.0°C and 6.9°C using the high and low thermal conductivity bounds, respectively, for the 1.0 m/s air velocity conditions. The extent of temperature nonuniformity is smaller than that estimated using the heat transfer limiting model approach.

It can be further noticed from Fig. 3 that the surface-centre temperature difference was negative for a small period during the earlier stages of drying. This is because the initial droplet temperature was slightly larger

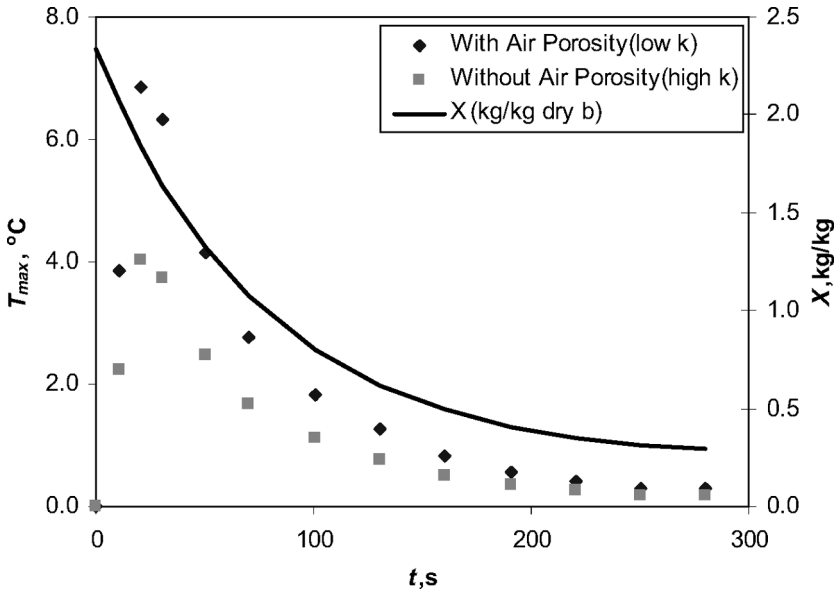


Figure 4. The surface-center temperature difference profiles for the 30 wt% (dry basis) skim milk droplet of 1.45 mm initial diameter and 28.6°C initial temperature during drying with hot air of 67.5°C dry-bulb temp, 23.4°C wet-bulb temp, and 1.0 m/s velocity.

than the wet-bulb temperature of surrounding air at the beginning of the process. The droplet surface temperature was, therefore, slightly reduced because the droplet surface temperature attempts to achieve the air wet-bulb temperature. The droplet had a negative surface-center temperature difference during this period due to the flow of heat from the center to the surface. The droplet should have experienced some evaporation during this surface temperature reduction period (or the initial wet-bulb temperature adjustment). This way, the assumption of no evaporation during the initial wet-bulb temperature adjustment cannot be generalised as done by the heat transfer limiting approach. The assumption of no evaporation is likely to produce an error in estimating the droplet surface temperature and the average particle temperature.

Figures 5 and 6 illustrate that the differences between the surface and the center temperatures were greater for the elevated air temperature conditions (refer sets two and three drying conditions). For instance, the difference was 5°C and 8°C for the high and low thermal conductivity bounds respectively when the air temperature was 87.1°C. For hot air of 106.6°C, the surface-center temperature differences were 7°C and 12°C

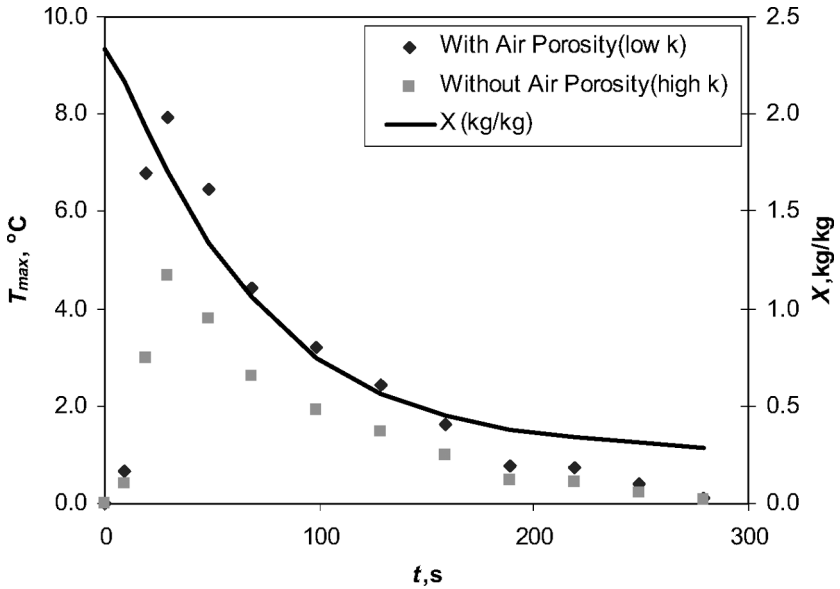


Figure 5. The surface-center temperature difference profiles for the 30 wt% (dry basis) skim milk droplet of 1.45 mm initial diameter and 31.8°C initial temperature during drying with hot air of 87.1°C dry-bulb temp, 28.5°C wet-bulb temp, and 0.45 m/s velocity (set two conditions).

using the high and low thermal conductivity bounds respectively. This shows that the air temperature significantly affects the surface properties of the droplet during drying. Furthermore, Figs. 3 to 6 show that the temperature differences are more significant during the earlier stages of drying, when the droplet moisture contents are reduced by 50%. The surface-center temperature differences are smaller during the later stages of drying, when the thermal conductivity may be important. This may mean that the thermal conductivity is not the only process controlling factor and drying may not be the heat transfer limiting. Moreover, the peaks in the surface-centre temperature differences are observed immediately after the wet-bulb temperature adjustment period. This finding is different from the heat transfer limiting approach as it assumes the uniform temperature period after the initial wet-bulb temperature adjustment.

The surface-center temperature differences (see Figs. 3 to 6) are comparatively greater for a model (Eq. (30)) which considered air porosity during the estimation of the mean thermal conductivity, especially during the earlier drying stages. This is because the model has integrated the

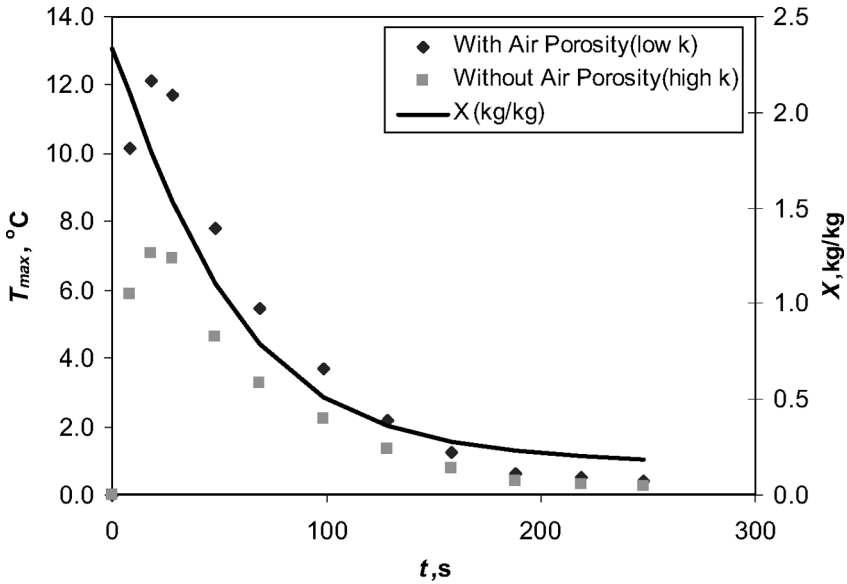


Figure 6. The surface-center temperature difference profiles for the 30 wt% (dry basis) skim milk droplet of 1.45 mm initial diameter and 30.8°C initial temperature during drying with hot air of 106.6°C dry-bulb temp, 32.0°C wet-bulb temp, and 0.45 m/s velocity (set three conditions).

porosity from the beginning of the simulation process. This concept predicted a low value for the initial mean thermal conductivity ($0.3 \text{ W} \cdot \text{m}^{-1} \cdot \text{K}^{-1}$) at the beginning of the drying process. The initial mean thermal conductivity at the beginning of drying should be the one ($0.5 \text{ W} \cdot \text{m}^{-1} \cdot \text{K}^{-1}$) predicted by a model, which does not consider the air phase (dispersed) in the droplet. The gradual change in the mean thermal conductivity of the droplet during drying should be similar to the one traced using a full line in Fig. 2. Therefore, the actual differences between the centre and the surface temperatures during the initial stages of drying should be very close to those predicted by the model which does not consider air porosity.

It is very clear from all the simulation results that the differences between the surface and the centre temperatures were not as large as predicted by the heat transfer limiting theory. In fact, the heat transfer limiting theory^[20] estimated the surface-core temperature differences by setting the crust thermal conductivity equal to $0.07 \text{ W} \cdot \text{m}^{-1} \cdot \text{K}^{-1}$, which is practically the thermal conductivity of completely dry skim milk powder in a packed bed.^[39] The low value of the thermal conductivity would of course predict the greater temperature differences. Furthermore, the

heat transfer limiting approach (a moving boundary model) did not consider the heat source term (the phase change effects) during modeling of the temperature characteristics. The heat transfer limiting theory would, therefore, expect the greater magnitude of the temperature distribution considering the nonevaporating situations.

Estimation of Biot numbers is also justified in the present study. Figures 7 to 9 illustrate the comparison of Biot numbers using both conventional and new definitions (Eqs. (6) and (11), respectively). It is important to note here that the Biot number characterized by Eq. (6) is not accounted for the evaporative nature of the droplets. The comparison was made for the same three sets of drying conditions used before. Biot numbers were evaluated using two thermal conductivity ranges predicted by two different models; one that does not consider air porosity and another that considers the air phase in the particle structure. This would show the lower and higher bounds of Biot numbers.

The lower and higher bounds of the Biot number profiles for the drying sets of one, two and three are illustrated in Figs. 7 to 9, respectively. The gradual change in Biot numbers during drying would pertain between these lower and higher bounds. The results show that Bi (new), which considered the evaporative nature of the droplet, were smaller than conventional Biot numbers (Bi) for the all sets of drying conditions. For

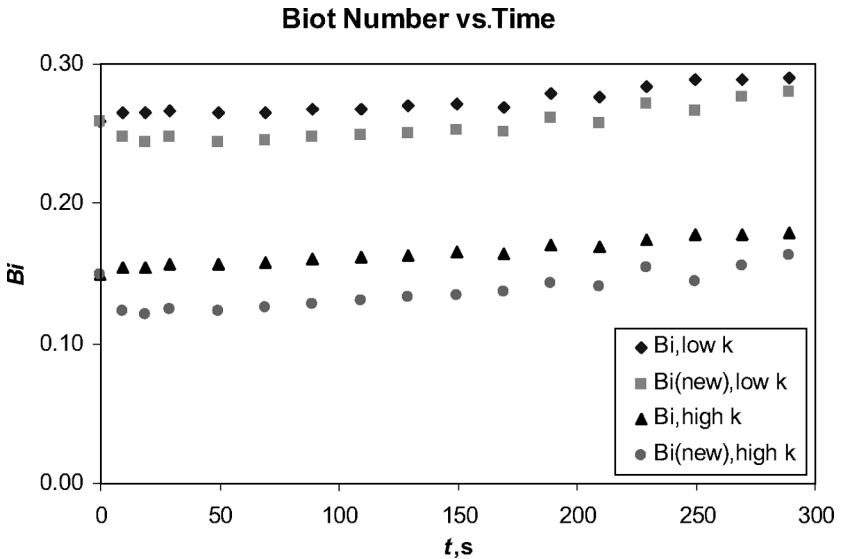


Figure 7. Biot number profiles for the 30 wt% (dry basis) skim milk droplets using set one conditions for the low and high thermal conductivity bounds.

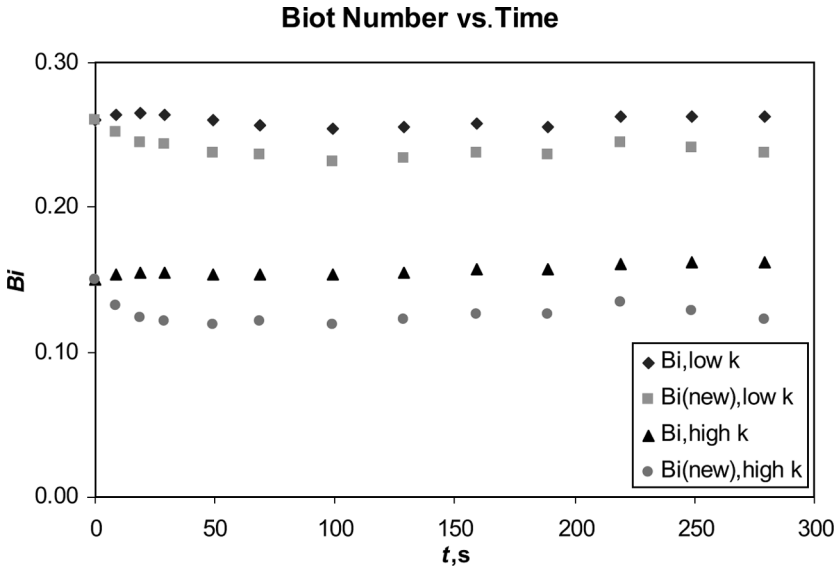


Figure 8. Biot number profiles for the 30 wt% (dry basis) skim milk droplets using set two conditions for the low and high thermal conductivity bounds.

instance, the Biot number at the beginning of the drying process was 0.15 for the 30 wt% skim milk droplets (refer to set one drying conditions) having an initial thermal conductivity of $0.5 \text{ W} \cdot \text{m}^{-1} \cdot \text{K}^{-1}$. At the end of drying, the mean thermal conductivity reduced to the value of $0.24 \text{ W} \cdot \text{m}^{-1} \cdot \text{K}^{-1}$. At this point, the final value of the conventional Biot number was 0.29 while it was 0.28 for the new Biot number. The difference between Bi and Bi (new) was small for the set one drying conditions but it was greater for the higher air temperature conditions (see Figs. 8 and 9). Bi (new) were significantly smaller than the conventional ones (Bi) for the set three (see Fig. 9). The reason is the increment in Bi (new) was smaller in comparison with conventional Biot number (Bi) due to the contribution of the second term on the right-hand side of the Eq. (11).

It can be observed from the Figs. 6 to 8 that Biot numbers at the end of drying were not as large as those predicted by the heat transfer limiting theory. For instance, the heat transfer limiting approach has estimated Biot numbers greater than the value of 1 for the final dried particles. In this work, Biot numbers for the final dried particles were much smaller. A smaller Biot number indicates smaller temperature nonuniformity within the droplet. Furthermore, the difference between the Biot number and its critical value was found to be smaller than that predicted by the heat transfer limiting theory at any stages of drying. This finding

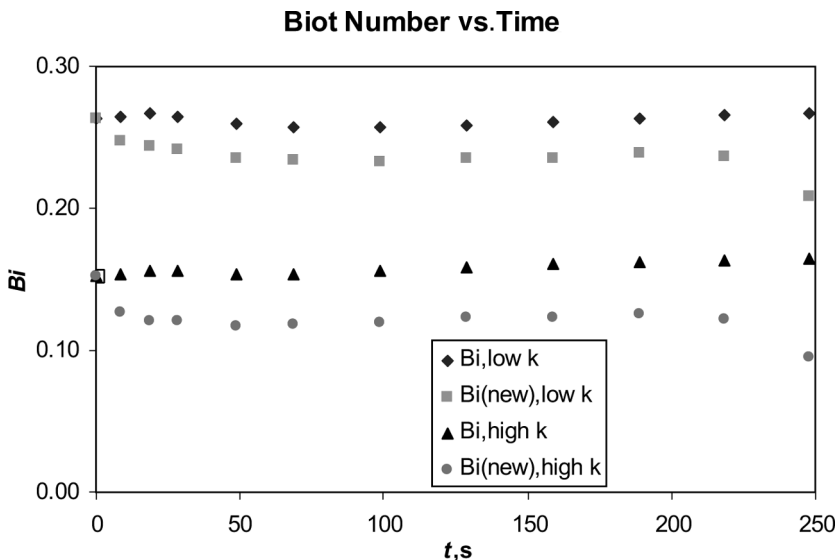


Figure 9. Biot number profiles for the 30 wt% (dry basis) skim milk droplets using set three conditions for the low and high thermal conductivity bounds.

supports the smaller temperature nonuniformity within the droplet during drying for the droplets found in the lab-scale experiments.

The drying experiments tested in this study were for single skim milk droplets having the initial diameter equal to 1.45 mm. In the industrial spray drying operations for manufacturing of skim milk powder, skim milk is usually sprayed with droplet diameter of the order of 0.2 mm, which is much smaller than those found in the lab-scale experiments. Experimental data for drying of such small size droplets are not available in the literature. Biot numbers are, however, estimated in this study for the 30 wt% skim milk droplets having the initial diameter of 0.20 mm (200 μm). The final diameter of the dried skim milk particle was assumed as 0.15 mm. Other drying conditions were kept the same as the conditions mentioned for the set one. The air phase was considered during calculating the mean thermal conductivity of the droplet. The average heat-transfer coefficient was estimated using the Ranz-Marshall correlation. The drying rate (surface area based) is assumed to be the same as that for the 1.45 mm size skim milk droplets; nevertheless the drying rates for the 0.2 mm size droplets would be higher. This later concept was confirmed by calculating the mass-transfer coefficients. The mass transfer coefficient estimated for the 0.2 mm size droplets was 0.484 m/s, which is bigger than the one for the 1.45 mm size skim milk droplets

(0.107 m/s) indicating that the smaller droplets should have greater mass flux per unit area. Note that Bi (new) would be even smaller for the higher drying rates conditions. All other thermophysical properties for the 0.2 mm size droplets would be same as those for the 1.45 mm size skim milk droplets experiencing the same drying conditions.

The analysis has shown that the conventional Bi at the beginning of the process was 0.07, while it was 0.11 at the end of drying, which is close to the critical value. The new definition of Biot number yielded Bi (new) equal to 0.07 at the beginning and 0.09 at the end of drying. The simulation shows that Biot numbers were either smaller or very close to its critical value of 0.1. Therefore, it is reasonable to say that the uniform temperature assumption can be used for modeling the temperature-time profiles of the skim milk droplets having size found in the industries. The uniform temperature assumption allows a CFD simulation of spray drying to be conducted more easily and indeed more efficiently.

CONCLUSIONS

The fundamental aspects of modeling for the droplet drying process were discussed in this article. A mathematical analysis is provided here for estimating the temperature distribution within a skim milk droplet during spray drying. The analysis in this paper shows that the Biot number and hence the temperature nonuniformity are significantly influenced by the drying rate, the surface temperature, the gas temperature, the droplet size and the average heat transfer coefficient together with the mean thermal conductivity of the droplet. Moreover, the analysis illustrates that the thermal conductivity of the particle may not be the only process-controlling factor and the droplet drying process may not be the heat transfer limiting process. The present study shows that the heat transfer limiting approach is more likely to exaggerate the surface-center temperature differences. Simulation conducted in this work exemplifies that the surface-center temperature differences were small for the skim milk droplets tested. Furthermore, Biot numbers and the difference between the Biot number and its critical value were found to be small, indicating the approximate temperature uniformity. The newly defined Biot numbers, which considered the evaporative nature of the droplets, were smaller than the conventional Biot numbers, signifying smaller temperature nonuniformity within the droplets under drying conditions. For small skim milk droplets found in the industries, Biot numbers were conservatively estimated to be smaller than the critical value. Based on these results, it may be said that the assumption of uniform internal temperature is a reasonable assumption for modeling the drying of small moist

droplets in a spray dryer, as far as prediction of the average droplet temperature and water content is concerned.

NOMENCLATURE

A_p	Surface area of single droplet or particle (m^2)
Bi	Biot number
Bi (new)	New Biot number
C_p	Specific heat ($\text{J}/\text{kg} \cdot \text{K}$)
d_p	Diameter of droplet or particle (m)
\bar{E}_v	Volume-based drying rate ($\text{kg}/\text{m}^3 \cdot \text{s}$)
h	Heat transfer coefficient ($\text{W}/\text{m}^2 \cdot \text{K}$)
h^*	Equivalent heat transfer coefficient ($\text{W}/\text{m}^2 \cdot \text{K}$)
ΔH_v	Latent heat of vaporization (J/kg)
m	Mass (kg)
\hat{N}_v	Area-based drying rate ($\text{kg}/\text{m}^2 \cdot \text{s}$)
r	Instantaneous droplet radius (m)
R	Droplet radius (m)
t	Time (s)
T	Temperature (K)
T_{wb}	Wet-bulb temperature of drying air (K)
w_0	Droplet initial water mass fraction (kg water/kg total)
w_b	Droplet bounded water mass fraction (kg water/kg total)

Greek Symbols

α	Thermal diffusivity (m^2/s)
ε	Volume fraction
ω	Mass fraction
ρ	Density (kg/m^3)

Subscripts

b	Bulk drying medium phase
c	Center conditions
p	Particle, droplet
s	Solid, surface
sat	Saturated conditions
v	Vapor
w	Water

ACKNOWLEDGMENTS

The authors would like to thank Dr. S.X.Q. Lin for providing the experimental measurements on drying of the single skim milk droplets. The first

author is the recipient of the University of Auckland Ph.D. scholarship and the third author is the recipient of the School of Engineering Ph.D. fee-waiver scholarship. We appreciate this funding.

REFERENCES

1. Birchal, V.S.; Passos, M.L.; Wildhagen, G.R.S.; Mujumdar, A.S. Effect of spray dryer operating variables on the whole milk powder quality. *Drying Technology* **2005**, *23* (3), 611–636.
2. Huang, L.X.; Kumar, K.; Mujumdar, A.S. Simulation of a spray dryer fitted with a rotary disk atomizer using a three dimensional computational fluid dynamic model. *Drying Technology* **2004**, *21* (3), 385–412.
3. Huang, L.X.; Kumar, K.; Mujumdar, A.S. A parametric study of the gas flow patterns and drying performance of co-current spray dryer: Results of a computational fluid dynamics study. *Drying Technology* **2003**, *21* (6), 957–978.
4. Huang, L.X.; Kumar, K.; Mujumdar, A.S. Use of computational fluid dynamics to evaluate alternative spray drying chamber configurations. *Drying Technology* **2003**, *21* (3), 385–412.
5. Fletcher, D.; Guo, B.; Harvie, D.; Langrish, T.; Nijdam, J.; Williams, J. What is important in the simulation of spray dryer performance and how do current CFD models perform. In *3rd International Conference on CFD in the Minerals and Process Industries*; Melbourne, Australia: CSIRO.
6. Parti, M.; Palancz, B. Mathematical model for spray drying. *Chemical Engineering Science* **1974**, *29* (2), 355–362.
7. Wijnhuizen, A.E.; Kerkhof, P.J.A.M.; Bruin, S. Theoretical study of the inactivation of Phosphatase during spray drying of skim milk. *Chemical Engineering Science* **1979**, *34* (5), 651–660.
8. Bruin, S.; Luyben, K.C.A.M. Drying of food materials: A review of recent developments. In *Advances in Drying, Vol. 1*; Mujumdar, A.S., Ed.; Hemisphere: New York, 1980; 155–215.
9. Sano, Y.; Keey, R.B. The drying of a spherical particle containing colloidal material into a hollow sphere. *Chemical Engineering Science* **1982**, *37* (6), 881–889.
10. Cheong, H.W.; Jeffreys, G.V.; Mumford, C.J. A receding interface model for the drying of slurry droplets. *AIChE Journal* **1986**, *32*, 1334–1346.
11. Chen, P.; Pei, D.C.T. A mathematical model of drying processes. *International Journal of Heat and Mass Transfer* **1989**, *32* (2), 297–310.
12. Meerdink, G.; Riet, K.V. Prediction of product quality during spray drying. *Trans IChemE, Part C: Food and Bioproducts Processing* **1995**, *73*, 165–170.
13. Chen, X.D.; Xie, G.Z. Fingerprints of the drying behaviour of particulate or thin layer food materials established using a reaction engineering model. *Trans IChemE, Part C: Food and Bioproducts Processing* **1997**, *75*, 213–222.
14. Stevenson, M.J.H.R. Computational modeling of drying milk droplets. *Master's Thesis*, The University of Auckland, New Zealand, 1999.

15. Chen, X.D.; Pirini, W.; Ozilgen, M. The reaction engineering approach to modeling drying of thin layer of pulped kiwifruit flesh under conditions of small *Biot* numbers. *Chemical Engineering and Processing* **2001**, *40*, 311–320.
16. Langrish, T.A.G.; Kockel, T.K. The assessment of a characteristic drying curve for milk powder for use in computational fluid dynamics modeling. *Chemical Engineering Journal* **2001**, *84*, 69–74.
17. Zhang, J.; Datta, A.K. Some considerations in modeling of moisture transport in heating of hygroscopic materials. *Drying Technology* **2004**, *22* (8), 1983–2008.
18. Chen, X.D.; Lin, S.X.Q. Air drying of milk droplet during constant and time-dependent temperature-humidity conditions: Modeling of the drying characteristics. *AIChE Journal* **2005**, *51* (6), 1790–1799.
19. Chen, X.D.; Peng, X. Modified *Biot* number in the context of air-drying of small moist porous objects. *Drying Technology* **2005**, *23* (1–2), 83–103.
20. Farid, M. A new approach to modeling of single droplet drying. *Chemical Engineering Science* **2003**, *58* (13), 2985–2993.
21. Zbicinski, I.; Grabowski, S.; Strumillo, C.; Kiraly, L.; Krzanowski, W. Mathematical modeling of spray drying. *Computers & Chemical Engineering* **1988**, *12* (2–3), 209–214.
22. Zbicinski, I. Development and experimental verification of momentum, heat and mass transfer model in spray drying. *Chemical Engineering Journal* **1995**, *58* (2), 123–133.
23. Szentgyorgyi, S.; Molnar, K. Calculation of drying parameters for the penetrating evaporating front. In *Proc. 1st International Symposium on Drying*, Mujumdar, A.S., Ed.; Science Press: Princeton, NJ, 92–99.
24. Pitts, D.R.; Sissom, L.E. *Schaum's Outline of Theory and Problems of Heat Transfer*; McGraw Hill: New York, 1977.
25. Mujumdar, A.S. *Handbook of Industrial Drying*; Marcel Dekker: New York, 1987.
26. Incropera, F.P.; DeWitt, D.P. *Fundamentals of Heat and Mass Transfer*, 5th Ed; John Wiley: New York, 2002.
27. Lin, S.X.Q. Drying of single milk droplets. *Ph.D. Thesis*; The University of Auckland, New Zealand, 2004.
28. Lin, S.X.Q.; Chen, X.D. Changes in milk droplet diameter during drying under constant drying conditions investigated using the glass-filament method. *Trans IChemE, Part C: Food and Bioproducts Processing* **2004**, *82* (C3), 213–218.
29. Písecký, J. *Handbook of Milk Powder Manufacture*; Niro A/S: Copenhagen, 1997.
30. Reis, Jr., N.C.; Griffiths, R.F.; Mantle, M.D.; Gladden, L.F. Investigation of the evaporation of embedded liquid droplets from porous surfaces using magnetic resonance imaging. *International Journal of Heat and Mass Transfer* **2003**, *46*, 1279–1292.
31. Whitaker, S. Moisture transport mechanisms during the drying of granular porous media, In *Drying* **85**, Mujumdar, A.S., Ed.; Hemisphere: Washington, DC, 1985; 21–32.

32. Bramhall, G. Sorption diffusion in wood. *Wood Science* **1979**, *12*, 3–13.
33. Bylund, G. *Dairy Processing Handbook*; Tetra Pak Processing Systems AB: Lund, Sweden, 1995.
34. Choi, Y.; Okos, M.R. Effects of temperature and composition on the thermal properties of foods. In *Transport Phenomena: Food Engineering and Process Applications, Vol. 1*; Le Maguer, M., Jelen, P., Eds.; Elsevier, Applied Science Publishers: London, 1986; 93–101.
35. Rahman, S. *Food Properties Handbook*; CRC Press: Boca Raton, FL, 1995.
36. Krokida, M.K.; Maroulis, Z.B.; Rahman, M.S. A structural generic model to predict the effective thermal conductivity of granular materials. *Drying Technology* **2001**, *19* (9), 2277–2290.
37. Chen, X.D. Towards a comprehensive model based control of milk drying processes, *Drying Technology* **1994**, *12* (5), 1105–1130.
38. Smith, J.M.; Van Ness, H.C.; Abbott, M.M. *Introduction to Chemical Engineering Thermodynamics*; McGraw-Hill: New York, 1996.
39. Al-Dabagh, W. Experimental investigation of thermal properties of particulate food materials. *Master's Thesis*, The University of Auckland, New Zealand, 2000.